The 21th Cambridge Workshop on Cool Stars, Stellar Systems, and the Sun
Edited by A. S. Brun, J. Bouvier, P. Petit

A new generation of evolutionary and seismic solar models

Gaël Buldgen,[1,2] Patrick Eggenberger[1]

[1] Département d'Astronomie, Université de Genève, Chemin Pegasi 51, CH-1290 Versoix, Switzerland
[2] Institut d'Astrophysique et Géophysique de l'Université de Liège, Allée du 6 août 17,4000 Liège, Belgium

Abstract

The Sun is the most observed star in the Universe. Thanks to this privileged status, it plays a key calibrator role for stellar physics, acting as a laboratory to test fundamental physical ingredients used in theoretical computations. Therefore, any refinement of the recipe of solar models will impact the ingredients for all models of solar-type stars. Following the revision of the solar abundances by Asplund and collaborators in 2005, confirmed in 2009, 2015 and 2021, the standard recipe of solar models has been put under question regarding both microscopic and macroscopic ingredients. In this work, we will present results of new generations of both solar evolutionary and seismic models. We will show how evolutionary models taking into account the effects of rotation and magnetic fields can reproduce both the internal rotation, the lithium surface abundance and the helium abundance in the convective zone of the Sun. Furthermore, we will present a new approach to compute seismic solar models from iterative Ledoux discriminant inversions. We will show how such seismic models can be used to gain insights on the temperature gradient close to the base of the convective zone, where the robustness of opacity tables has been questioned. Combining both approaches will thus provide us with key constraints on the required revision of physical ingredients to solve the long lasting solar modeling problem that followed the abundance revision in the early 2000s.

1 Introduction

The Sun plays a central role in astrophysics. Thanks to the unparalleled observational constraints available, it serves as a laboratory for fundamental physics and a calibrator for stellar evolution. In this context, revising the procedure used in the computation of solar models and developing new approaches to pinpoint the limitations of the current generation of models is paramount. This is the approach presented in this work. We briefly discuss the results of two papers (Buldgen *et al.*, 2020; Eggenberger *et al.*, 2022) and outline how they are complementary in building a new generation of solar models and by association, of solar-like stars in general.

We start in Sect. 2 by describing the results of Eggenberger *et al.* (2022) regarding new evolutionary models reproducing simultaneously the solar internal rotation and photospheric lithium abundance. We show how these new non-standard solar models also improve the agreement with the helium mass fraction in the convective zone measured by helioseismology when the metallicity of Asplund *et al.* (2009) or Asplund *et al.* (2021) is used. While these models do not solve the whole solar problem, they offer some insight into the impact of angular momentum transport on the way we model the Sun. Moreover, they show the existence of a connection between lithium depletion and increase in helium abundance in the convective zone, that can be attributed to the inclusion of the transport of angular momentum.

The second half of the paper, starting in Sect. 3 describes the results of Buldgen *et al.* (2020) on iterated seismic models built from successive Ledoux discriminant inversions. The results of the inversions are discussed, as well as their link to the evolutionary model sof Sect. 2 and the consequences for future revisions of physical ingredients of solar models.

2 Solar evolutionary models

Solar evolutionary models are the most common solar models. They are computed by calibrating the initial parameters of a stellar evolutionary sequence and assuming a given history of the Sun. Therefore, various physical ingredients enter their computation, such as nuclear reaction rates, chemical mixture, equations of state, radiative opacities, transport of chemicals, formalism of convection, ... (See Basu & Antia (2008); Buldgen *et al.* (2019a); Christensen-Dalsgaard (2021) for a review and Buldgen *et al.* (2019b) for a test of these ingredients against helioseismic data and Salmon *et al.* (2021) against neutrino fluxes).

In most cases, these ingredients will be kept fixed for a given calibration procedure and observational constraints such as helioseismic, spectroscopic and neutrino data are used to study their impact on solar modelling. The conclusions drawn for solar models are often extended to other stars (solar-like and beyond), especially with the advent of space-based photometric missions dedicated to asteroseismology (Baglin *et al.*, 2009; Borucki *et al.*, 2010; Rauer *et al.*, 2014; Ricker *et al.*, 2015). In that sense, solar evolutionary models are key calibrators of the current and future generations of stellar models.

2.1 Standard and non-standard models

Standard solar models are the simplest calibrated solar evolutionary models. They only consider microscopic diffusion as the source of chemical transport in radiative zones, often neglecting the effects of radiative accelerations (which remains a good hypothesis for solar conditions, as shown by Turcotte *et al.* (1998)). Other physical ingredients will be the "standard ones", which have slightly evolved over time (see e.g. Christensen-Dalsgaard, 2021, for a review). The framework of the standard solar models consists in reproducing

at the solar age the current solar radius, metallicity provided by solar abundances tables and luminosity (or effective temperature) using a one solar mass model and calibrating its initial chemical composition (hydrogen mass fraction X and metal mass fraction Z) and the mixing length parameter of convection. This optimization problem thus has a unique solution and can be solved efficiently with local minimization algorithms.

While quite simplified, they are extensively used in detailed comparisons against data. Their popularity is also justified by the fact that they reproduce the solar interior quite well and thus confirmed our understanding of the dominant factors influencing solar evolution. Their agreement with helioseismic data also played a key role in the outcome of the solar neutrino problem.

However, standard solar models also showed clear limitations, stemming from the fact that they neglected the effects of rotation (thoroughly constrained by helioseismology) and are unable to reproduce the observed lithium depletion. The recent debate surrounding solar abundances (see Basu & Antia, 2008; Christensen-Dalsgaard, 2021) has also exposed some of the limitations of solar models and raised questions regarding their physical ingredients.

Non-standard solar models are essentially all evolutionary models including additional free parameters, either linked to convection, rotation or evolutionary history. In this context, the calibration of these additional free parameters requires additional constraints so that the problem remains well-posed, such as the photospheric lithium abundance or the position of the base of the solar convective envelope. Nevertheless, degeneracies remain as some constraints can be reproduced through different approaches. Some extended calibration procedures exploring various effects such as modifications of radiative opacities and nuclear reaction rates or the effects of planetary formation have been presented (see Mussack & Däppen, 2011; Ayukov & Baturin, 2017; Kunitomo & Guillot, 2021; Kunitomo *et al.*, 2022, and refs therein).

Here, we will focus on non-standard models including the effects of rotation. The internal rotation of the Sun is well-known (see e.g. Couvidat *et al.*, 2003) and an extended litterature has been dedicated to finding a suitable transport process capable of reproducing the flat rotation profile in the solar radiative interior (see e.g. Schatzman, 1993; Gough & McIntyre, 1998; Charbonnel & Talon, 2005; Eggenberger *et al.*, 2005; Pinçon *et al.*, 2016). Indeed, rotating models including only the effects of meridional circulation and shear instabilities lead to a high degree of radial differential rotation and are thus in strong disagreement with helioseismic data. In this work, we will present the results obtained for one of such candidates, the magnetic Tayler instability, presented in Spruit (2002). We refer to Eggenberger *et al.* (2022) for details about the formalism and implementation.

Models are computed with the Geneva Evolution Code (GENEC, Eggenberger *et al.*, 2008), using the hypothesis of shellular rotation Zahn (1992). The transport of both angular momentum and chemicals is computed consistently during the evolution, taking into account meridional currents, shear instability, and the magnetic Tayler instability. The equation describing the internal angular momentum transport (Mathis & Zahn, 2004) in the solar radiative zone is

$$\rho \frac{\mathrm{d}}{\mathrm{d}t}\left(r^2\Omega\right)_{M_r} = \frac{1}{5r^2}\frac{\partial}{\partial r}\left(\rho r^4 \Omega U(r)\right) + \frac{1}{r^2}\frac{\partial}{\partial r}\left(\rho(D_{\rm shear}+\nu_{\rm T})r^4\frac{\partial \Omega}{\partial r}\right), \quad (1)$$

with r, the radius, $\rho(r)$, the mean density on an isobar and $\Omega(r)$, the mean angular velocity. $U(r)$ is the radial dependence of the velocity of the meridional circulation in the radial direction, following the expression of Maeder & Zahn (1998) and includes the effect of chemical gradients and horizontal turbulence. $D_{\rm shear}$ is the diffusion coefficient for angular momentum transport by the shear instability, here following Talon & Zahn (1997) to remain consistent with Maeder & Zahn (1998). These expressions for $U(r)$ and $D_{\rm shear}$ do not include free parameters and horizontal turbulence is modelled using the prescription of Maeder (2003), where the uncertainty on this coefficient is reflected in the constant n appearing in its mathematical expression. The quantity $\nu_{\rm T}$ is the viscosity associated with angular momentum transport by the magnetic Tayler instability, following Spruit (2002)

$$\nu_{\rm T} = r^2 \Omega q^2 \left(\frac{\Omega}{N_{\rm eff}}\right)^4 , \quad (3)$$

where $q = -\frac{\partial \ln \Omega}{\partial \ln r}$ and $N_{\rm eff}$ is an effective Brunt-Väisälä frequency defined with

$$N^2_{\rm eff} = \frac{\eta}{K} N^2_T + N^2_\mu , \quad (4)$$

where N_T and N_μ are the thermal and chemical composition terms of the Brunt-Väisälä frequency, and η and K are the magnetic and thermal diffusivities. This magnetic transport is active only if the shear parameter q is larger than a threshold $q_{\rm min}$ defined with

$$q_{\rm min} = \left(\frac{N_{\rm eff}}{\Omega}\right)^{7/4}\left(\frac{\eta}{r^2 N_{\rm eff}}\right)^{1/4} . \quad (5)$$

A very efficient angular momentum transport leading to a flat radial rotation profile is assumed in convective zones and the braking of the stellar surface by magnetized winds is included following Matt *et al.* (2015).

The same transport efficiency by the shear instability is taken for angular momentum and chemicals with the $D_{\rm shear}$ coefficient of Talon & Zahn (1997). The transport of chemicals through both vertical advection and horizontal turbulence is described by the diffusion coefficient $D_{\rm eff} = |rU(r)|^2/30D_{\rm h}$ (Chaboyer & Zahn, 1992), with $D_{\rm h}$ the coefficient for horizontal turbulence of Maeder (2003). The direct transport of chemical elements by the magnetic Tayler instability is taken from Spruit (2002)

$$D_{\rm T} = r^2 \Omega q^4 \left(\frac{\Omega}{N_{\rm eff}}\right)^6 , \quad (6)$$

whenever the shear is sufficient for the instability to be active. Consequently, the transport of chemical elements is directly and self-consistently computed from the rotational and magnetic properties of the model without any additional free parameter.

As shown in Fig. 1, the inclusion of this instability allows to extract angular momentum from the interior and leads to a close to rigid rotation profile down to the inner core. The spin-up of the inner core is due to the inhibiting effects of molecular weight gradients on the instability. Therefore, a

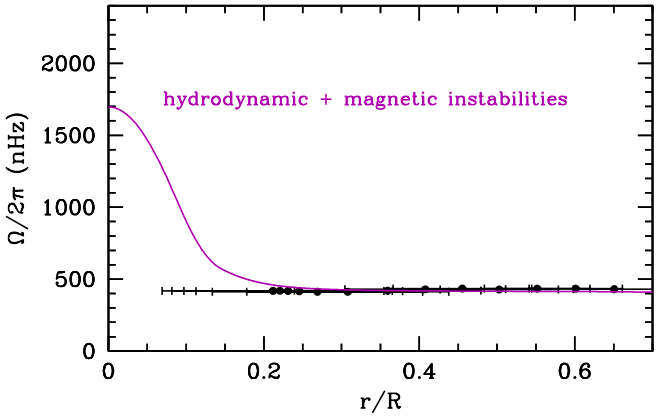

Figure 1: Rotation profile in the solar radiative zone of a model computed with the abundances of Asplund *et al.* (2009) with both hydrodynamic and magnetic instabilities. Black dots are the helioseismic measurements of Couvidat *et al.* (2003).

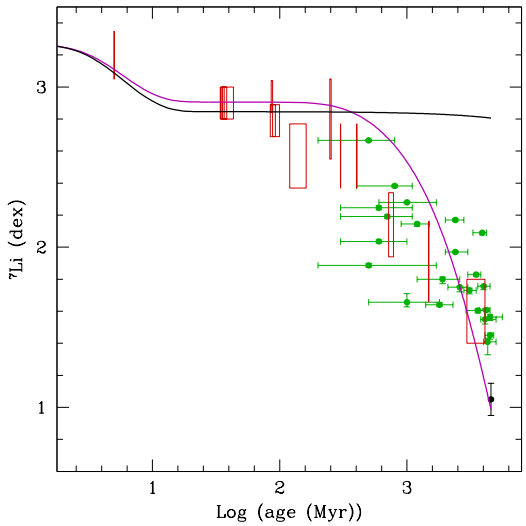

Figure 2: Photospheric lithium abundance as a function of time for the standard (black) and non-standard (purple) solar models of Eggenberger *et al.* (2022). The black dot indicates the solar value of Asplund *et al.* (2009). Green dots show the lithium abundances of solar-type stars by Carlos *et al.* (2019) (for stars younger than the Sun). Red boxes show the surface lithium abundances in young open clusters from Dumont *et al.* (2021).

key feature of the magnetic Tayler instability is the faster rotating solar core.

The exact physical nature of the angular momentum transport mechanism is still unknown, and it is worth noting that the detection of solar gravity modes would play a decisive role in this issue by unraveling the rotation of the inner core. Subsequently, this would also influence the modelling of solar-like stars in general.

2.2 Rotation - helium - lithium relation

A key result found by Eggenberger *et al.* (2022) is that the inclusion of additional transport of angular momentum leads to an additional transport of chemicals at the BCZ. This effect is due to the regulation of the shear instability by the magnetic Tayler instability, which leads to a small but significant transport of chemicals. This transport leads to an additional depletion of lithium, in agreement with the observed photospheric abundance, as shown in Fig. 2. Eggenberger *et al.* (2022) showed that the depletion generated by the combined instabilities also reproduced the trend observed in young solar twins in open clusters (Dumont *et al.*, 2021). They also tested the impact of adding adiabatic overshooting to reproduce the position of the BCZ as inferred from helioseismic data and showed that this significantly increased the depletion in PMS.

In addition to leading to an increased depletion of lithium, it was also shown that the inclusion of macroscopic transport as a result of angular momentum transport increased significantly the helium abundance in the CZ, bringing the value for models with Asplund *et al.* (2021) abundances in agreement with the helioseismic value and thus solving one aspect of the solar problem. This is illustrated in Fig 3 for a standard model and a model including a full tratement of angular momentum transport. Eggenberger *et al.* (2022) also showed that this relation between lithium and helium was independent of the process involved, as long as it was linked to an additional diffusive transport at the BCZ. Buldgen *et al.* (2023) extended this study to high-metallicity models and showed that this increased the helium mass fraction in the convective envelope to a level of marginal agreement/disagreement with the helioseismic value depending on the shape of the diffusion coefficient.

Overall, this new generation of solar models demonstrates the need to correctly depict angular momentum transport and its impact on the transport of chemicals. Including the effect of both hydrodynamical instabilities and the magnetic Tayler instability leads to a consistent rotation profile in the solar interior and simultaneously reproduces the correct lithium depletion as well as improving the agreement of Asplund *et al.* (2021) models regarding the helium mass fraction.

3 Solar seismic models

Thanks to the high quality of helioseismic data, it is possible to reconstruct the internal structure of the Sun as seen by the global acoustic oscillations. This requires a reference model (usually a calibrated evolutionary model) which is then iteratively corrected for the differences observed from helioseismic inversions. Various techniques and approaches have been used in the litterature, also discussing the inclusion of non-seismic constraints such as neutrino fluxes or luminosity in the procedure (Shibahashi & Takata, 1996; Gough, 2004).

3.1 Iterated Ledoux discriminant inversions

The seismic models presented here are taken from Buldgen *et al.* (2020) and built from successive inversions of the Ledoux discriminant. This approach has been shown to provide excellent agreement in all other seismic indicators available (frequency ratios, sound speed, density and entropy proxy inversions). The Ledoux discriminant profile obtained

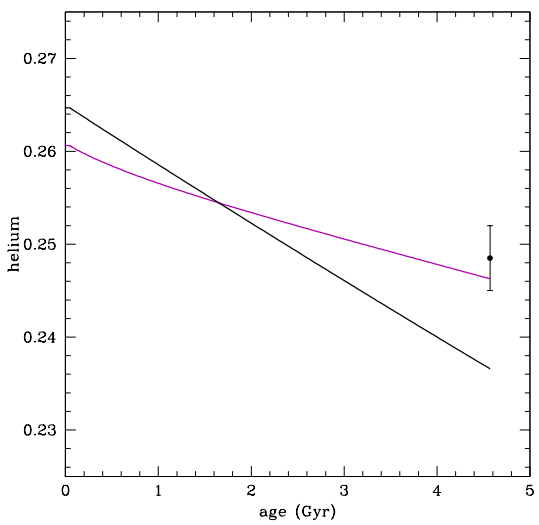

Figure 3: Evolution of the surface helium mass fraction as a function of time for a standard solar model (black) and a non-standard model including angular momentum transport (purple), both computed with the Asplund *et al.* (2009) abundances. The dark dot indicates the helioseismic value from Basu & Antia (1995).

after convergence is fully independent from the reference solar model used in the inversion procedure. The inversion method used is the SOLA method (Pijpers & Thompson, 1994), using the Ledoux discriminant kernels (See Buldgen *et al.*, 2020, for a full description).

The procedure requires approximately 7 iterations before the corrections are negligible and beyond the resolution of the inversion. A full structure is integrated after every iteration, in a similar fashion to the approach of Antia (1996). Fig 4 illustrates the iteration procedure and shows the final seismic profile at the end of the reconstruction. The final seismic profile is model independent, and bears no trace of the initial conditions, except below $0.08 R_{\odot}$ as this region is not strongly constrained by the inversion.

Buldgen *et al.* (2020) have shown that this procedure provided seismic solar models showing agreement overall within 0.1% in the solar radiative regions with all inversions of solar structure. Therefore, the models can be considered very high quality although further refinements could be brought by using non-linear iterative inversions to erase the last remaining discrepancies (Corbard *et al.*, 1999).

3.2 Implications for revision of physical ingredients of Solar models

A key feature of the reconstruced model of Buldgen *et al.* (2020) is the significant modification of the Ledoux discriminant in the vicinity of the solar BCZ. This is seen for every model and leads to the same corrected profile after reconstruction. The Ledoux discriminant profile can be separated into its thermal and chemical composition contribution, as in Eq. 8.

$$\mathrm{A} = \frac{1}{\Gamma_1}\frac{d\ln \mathrm{P}}{d\ln \mathrm{r}} - \frac{d\ln\rho}{d\ln \mathrm{r}} = \frac{\mathrm{r}\delta}{\mathrm{H_P}}\left(\nabla_{\mathrm{ad}} - \nabla + \frac{\phi}{\delta}\nabla_{\mu}\right) \quad (7)$$

$$= \mathrm{A}^{\mathrm{T}} + \mathrm{A}^{\mu}, \quad (8)$$

with P the local pressure, ρ the local density, $\Gamma_1 = \left.\frac{\partial \ln \mathrm{P}}{\partial \ln \rho}\right|_{\mathrm{S}}$ the first adiabatic exponent and S the entropy, r the position of the layer in the model, $\delta = \frac{-\partial \ln \rho}{\partial \ln \mathrm{T}}$, $\mathrm{H_P} = \frac{-\mathrm{dr}}{\mathrm{d}\ln \mathrm{P}}$ the local pressure scale height, ∇_{ad} the adiabatic temperature gradient, $\nabla = \frac{\mathrm{d}\ln \mathrm{T}}{\mathrm{d}\ln \mathrm{P}}$ the temperature gradient, $\phi = \frac{\partial \ln \rho}{\partial \ln \mu}$ and $\nabla_{\mu} = \frac{\mathrm{d}\ln \mu}{\mathrm{d}\ln \mathrm{P}}$ the mean molecular weight gradient. We split A in its chemical and thermal components, A^{μ} and A^{T} to isolate the regions where the effects of chemical composition gradients dominate.

One can then see the regions where each one will dominate. This is illustrated in Fig 5 where the dashed lines illustrate the thermal contribution and the full line the total Ledoux discriminant profile. The differences between the two indicate where the effects of mean molecular weight gradients, which unsurprisingly become significant just below the convective zone, where the effects of settling are important. From Fig. 5, we can also see a stringent difference between the Standard Solar Model (SSM) and the model including macroscopic transport. In the latter, the thermal contribution clearly dominates the profile, as a result of the efficient mixing at the BCZ that erases the mean molecular weight gradients built by microscopic diffusion.

This result can be used to infer a correction on the temperature gradient of solar models. Indeed, due to the effects of rotation, or even dynamical shear from turning convective elements, the effects of microscopic diffusion can be expected to be erased. Consequently, most of the correction seen in the Ledoux discriminant profile can be attributed to corrections in temperature gradient. In turn, these corrections can be related to either thermalization of the convective elements beyond the Scharzschild boundary of the model (see e.g. Rempel, 2004; Christensen-Dalsgaard *et al.*, 2011; Zhang, 2014; Baraffe *et al.*, 2022) or opacity corrections (see e.g. Christensen-Dalsgaard *et al.*, 2009; Pradhan & Nahar, 2009; Bailey *et al.*, 2015; Nahar & Pradhan, 2016a; Blancard *et al.*, 2016; Nahar & Pradhan, 2016b).

4 Conclusion

In this paper, we briefly discussed the results presented in Eggenberger *et al.* (2022) and Buldgen *et al.* (2020) regarding new evolutionary and seismic solar models. The results of both studies are complementary in nature, as they shed lights on various main aspects of the physics of the Sun. The new evolutionary models tackle macroscopic aspects of solar structure and evolution, by showing how angular momentum transport can have an important impact on our understanding of the Sun. The relation between lithium, helium and internal rotation underlines the importance of moving away from the standard solar model recipe. Similarly, the new seismic solar models presented in Buldgen *et al.* (2020) pave the way for further analysis of the Sun, looking at thermal gradients and potentially guiding future revision of both macrophysical and microphysical ingredients. In the context of the solar problem, such revisions have been extensively discussed theoretically and experimentally.

Ultimately these uncertainties are not only present for the Sun but also for other stars who will be affected by the prescriptions used for angular momentum transport and

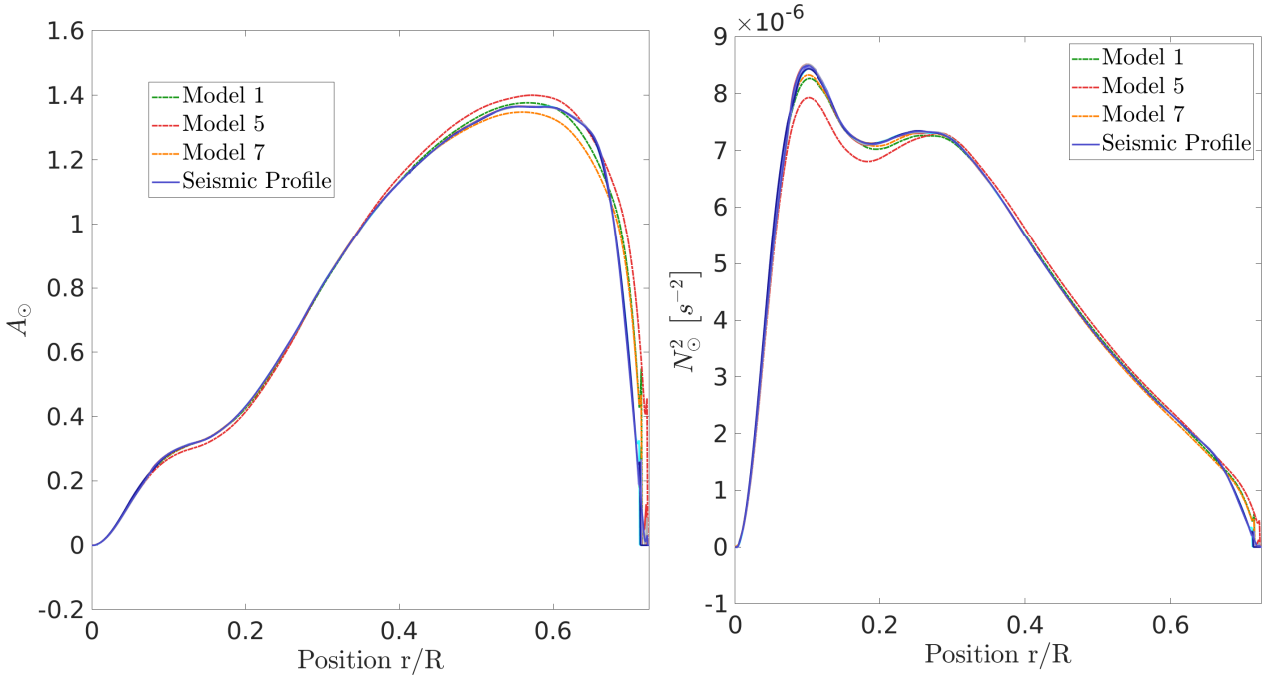

Figure 4: Left panel: Ledoux discriminant profile for some reference models of Buldgen *et al.* (2020) and the reconstructed seismic profile in blue. Right panel: same for the Brunt-Väisälä frequency profile.

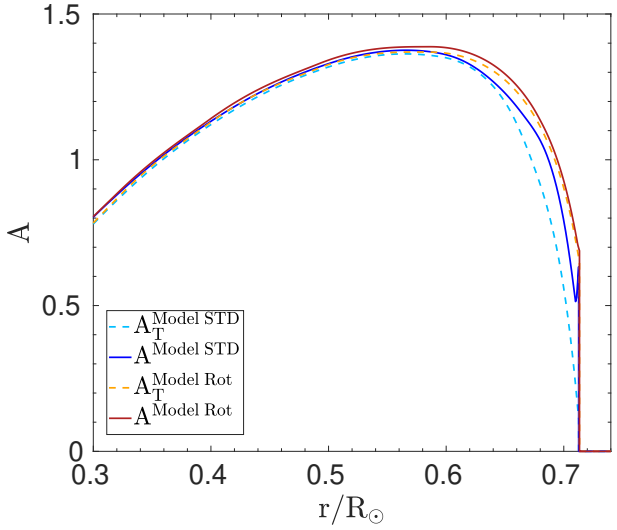

Figure 5: Ledoux discriminant profile of a Standard (blue) and Non-standard solar model (red) and their respective (light blue and orange) thermal component of the Ledoux discriminant (see Eq. 8).

revisions of thermal gradients near convective boundaries. Therefore, the results we derived for the Sun will likely trickle down to other stars in the Universe.

Acknowledgments

GB acknowledges fundings from the SNF AMBIZIONE grant No 185805 (Seismic inversions and modelling of transport processes in stars). PE has received fundings from the European Research Council (ERC) under the European Union's Horizon 2020 research and innovation programme (grant agreement No 833925, project STAREX). We acknowledge support by the ISSI team "Probing the core of the Sun and the stars" (ID 423) led by Thierry Appourchaux.

References

Antia, H. M. 1996, A&A, 307, 609.
Asplund, M., Amarsi, A. M., & Grevesse, N. 2021, A&A, 653, A141.
Asplund, M., Grevesse, N., Sauval, A. J., & Scott, P. 2009, ARA&A, 47, 481.
Ayukov, S. V. & Baturin, V. A. 2017, Astronomy Reports, 61, 901.
Baglin, A., Auvergne, M., Barge, P., Deleuil, M., Michel, E., *et al.* 2009, In *IAU Symposium*, edited by F. Pont, D. Sasselov, & M. J. Holman, *IAU Symposium*, vol. 253, pp. 71–81.
Bailey, J. E., Nagayama, T., Loisel, G. P., Rochau, G. A., Blancard, C., *et al.* 2015, Nature, 517, 3.
Baraffe, I., Constantino, T., Clarke, J., Le Saux, A., Goffrey, T., *et al.* 2022, A&A, 659, A53.
Basu, S. & Antia, H. M. 1995, MNRAS, 276, 1402.
Basu, S. & Antia, H. M. 2008, Phys. Rep., 457, 217.

Blancard, C., Colgan, J., Cossé, P., Faussurier, G., Fontes, C. J., *et al.* 2016, Phys. Rev. Lett., 117, 249501.
Borucki, W. J., Koch, D., Basri, G., Batalha, N., Brown, T., *et al.* 2010, Science, 327, 977.
Buldgen, G., Eggenberger, P., Baturin, V. A., Corbard, T., Christensen-Dalsgaard, J., *et al.* 2020, A&A, 642, A36.
Buldgen, G., Eggenberger, P., Noels, A., Scuflaire, R., Amarsi, A. M., *et al.* 2023, A&A, 669, L9.
Buldgen, G., Salmon, S., & Noels, A. 2019a, Frontiers in Astronomy and Space Sciences, 6, 42.
Buldgen, G., Salmon, S. J. A. J., Noels, A., Scuflaire, R., Montalban, J., *et al.* 2019b, A&A, 621, A33.
Carlos, M., Meléndez, J., Spina, L., dos Santos, L. A., Bedell, M., *et al.* 2019, MNRAS, 485, 4052.
Chaboyer, B. & Zahn, J.-P. 1992, A&A, 253, 173.
Charbonnel, C. & Talon, S. 2005, Science, 309, 2189.
Christensen-Dalsgaard, J. 2021, Living Reviews in Solar Physics, 18, 2.
Christensen-Dalsgaard, J., di Mauro, M. P., Houdek, G., & Pijpers, F. 2009, A&A, 494, 205.
Christensen-Dalsgaard, J., Monteiro, M. J. P. F. G., Rempel, M., & Thompson, M. J. 2011, MNRAS, 414, 1158.
Corbard, T., Blanc-Féraud, L., Berthomieu, G., & Provost, J. 1999, A&A, 344, 696.
Couvidat, S., García, R. A., Turck-Chièze, S., Corbard, T., Henney, C. J., *et al.* 2003, ApJL, 597, L77.
Dumont, T., Palacios, A., Charbonnel, C., Richard, O., Amard, L., *et al.* 2021, A&A, 646, A48.
Eggenberger, P., Buldgen, G., Salmon, S. J. A. J., Noels, A., Grevesse, N., *et al.* 2022, Nature Astronomy, 6, 788.
Eggenberger, P., Maeder, A., & Meynet, G. 2005, A&A, 440, L9.
Eggenberger, P., Meynet, G., Maeder, A., Hirschi, R., Charbonnel, C., *et al.* 2008, Ap&SS, 316, 43.
Gough, D. 2004, In *Equation-of-State and Phase-Transition in Models of Ordinary Astrophysical Matter*, edited by V. Celebonovic, D. Gough, & W. Däppen, *American Institute of Physics Conference Series*, vol. 731, pp. 119–138.
Gough, D. O. & McIntyre, M. E. 1998, Nature, 394, 755.
Kunitomo, M. & Guillot, T. 2021, A&A, 655, A51.
Kunitomo, M., Guillot, T., & Buldgen, G. 2022, A&A, 667, L2.
Maeder, A. 2003, A&A, 399, 263.
Maeder, A. & Zahn, J.-P. 1998, A&A, 334, 1000.
Mathis, S. & Zahn, J. P. 2004, A&A, 425, 229.
Matt, S. P., Brun, A. S., Baraffe, I., Bouvier, J., & Chabrier, G. 2015, ApJL, 799, L23.
Mussack, K. & Däppen, W. 2011, ApJ, 729, 96.
Nahar, S. N. & Pradhan, A. K. 2016a, Phys. Rev. Lett., 116, 235003.
Nahar, S. N. & Pradhan, A. K. 2016b, Phys. Rev. Lett., 117, 249502.
Pijpers, F. P. & Thompson, M. J. 1994, A&A, 281, 231.
Pinçon, C., Belkacem, K., & Goupil, M. J. 2016, A&A, 588, A122.
Pradhan, A. K. & Nahar, S. N. 2009, In *Recent Directions in Astrophysical Quantitative Spectroscopy and Radiation Hydrodynamics*, edited by I. Hubeny, J. M. Stone, K. MacGregor, & K. Werner, *American Institute of Physics Conference Series*, vol. 1171, pp. 52–60.
Rauer, H., Catala, C., Aerts, C., Appourchaux, T., Benz, W., *et al.* 2014, Experimental Astronomy, 38, 249.
Rempel, M. 2004, ApJ, 607, 1046.
Ricker, G. R., Winn, J. N., Vanderspek, R., Latham, D. W., Bakos, G. Á., *et al.* 2015, Journal of Astronomical Telescopes, Instruments, and Systems, 1, 014003.
Salmon, S. J. A. J., Buldgen, G., Noels, A., Eggenberger, P., Scuflaire, R., *et al.* 2021, A&A, 651, A106.
Schatzman, E. 1993, A&A, 279, 431.
Shibahashi, H. & Takata, M. 1996, PASJ, 48, 377.
Spruit, H. C. 2002, A&A, 381, 923.
Talon, S. & Zahn, J. P. 1997, A&A, 317, 749.
Turcotte, S., Richer, J., Michaud, G., Iglesias, C. A., & Rogers, F. J. 1998, ApJ, 504, 539.
Zahn, J.-P. 1992, A&A, 265, 115.
Zhang, Q. S. 2014, ApJL, 787, L28.